Laser-Assisted Formation of Porous Silicon in Diverse Fluoride Solutions: Hexafluorosilicate Deposition

Lynne Koker,[†,‡] Anja Wellner,[§,||] Paul A. J. Sherratt,[†] Rolf Neuendorf,[§,⊥] and Kurt W. Kolasinski*[,†,▽]

School of Chemistry, Nanoscale Physics Research Laboratory, and the School of Physics and Astronomy, The University of Birmingham, Edgbaston, Birmingham, B15 2TT, U.K.

Received: August 18, 2001; In Final Form: November 6, 2001

Photoluminescent porous silicon has been produced in a variety of etchants using laser-assisted etching of silicon without an applied potential. Porous silicon (por-Si) produced from etchants containing K^+, Cs^+, or Rb^+ can have cubic crystallites of hexafluorosilicate on top of and embedded in the porous silicon film. These are formed during etching from the metal ion and the etch product, SiF_6^{2-}, via heterogeneous nucleation and growth. The photoluminescence of the hexafluorosilicate-coated por-Si on excitation with UV light is blue-shifted (590−610 nm), as compared to porous silicon that shows red photoluminescence (∼640 nm), even though the pure hexafluorosilicates exhibit no photoluminescence of their own.

1. Introduction

Research into the production and properties of porous silicon (por-Si) has grown exponentially in recent years. Initial excitement surrounded por-Si because it represents an inexpensive and easily prepared form of nanostructured silicon. Quantum confinement effects are prominent in por-Si, which has led to a range of studies into its optoelectronic properties. Whereas an explanation of Canham's observation of visible light emission[1] has motivated most of the work on por-Si, increasingly, interest has developed in por-Si as a bio-compatible material[2−4] and as a component of chemical and biochemical sensors.[5−10]

Quantum confinement is undoubtedly linked to the origin of visible photoluminescence (PL) from por-Si, though debate on a complete description continues.[11,12] High porosity is necessary for efficient visible PL. However, an explanation based on quantum size effects alone does not explain all observations (including wavelength, intensity, evolution in time, quenching, and the effects of incorporating other materials). Surface species, surface states, the wavelength of light used in photoassisted etching, and pore structure play a role, as reflected in recent discussions.[13−17] Immersion of por-Si in solutions of copper, silver, or gold ions, which are reduced to the metals,[18,19] quenches PL; however, other ions with lower (negative) standard electrode potentials do not. The PL of iron-passivated por-Si shows two bands,[20] and platinum-plated por-Si is photoluminescent, with a peak wavelength around 700 nm.[21] Erbium-doped por-Si exhibits PL at 1.54 μm arising from the Er^{3+} and a broad band from 500 to 900 nm due to the por-Si.[22−24]

Growing attention has been directed toward the creation of stable deposits of specific materials on the surfaces of por-Si. It is necessary to refer to two distinct surface regions: (a) the top of the por-Si layer and (b) the surface of the skeleton within the porous layer. To distinguish unambiguously between these two surfaces, we refer to them as the external surface and the internal surface, respectively. Special applications such as sensors, biomaterials, and electronic and optical devices require a well-defined stable surface. Hérino has recently reviewed composite structures formed from por-Si by the deposition of different materials onto the internal surface.[25] Polymers and metals have been successfully incorporated, and the techniques employed include chemical vapor deposition, impregnation of pores with a liquid, and electrochemical processes where the material to be deposited is formed in the pores. The amount of material deposited ranges from a submonolayer on the silicon to total filling of the pores. Passivation and functionalization of silicon and por-Si by deposition of organic mono- and submonolayers bonded directly to the silicon have been reviewed by Buriak.[26,27] The use of por-Si as a biological or chemical sensor necessitates a technique to deposit a specific and characterized layer over the porous skeleton.[9,28−30] One of the obstacles to passivating and functionalizing por-Si is the difficulty of reproducibly and homogeneously incorporating the deposit into the pores. The latter represents one reason we have attempted to grow por-Si and simultaneously deposit a dielectric layer.

A passivating layer of K_2SiF_6 has been observed during chemomechanical polishing of silica in the presence of KHF_2. Boyle et al.[31] report an IR spectrum in which the main bands of the thin-film spectrum agree with the bulk spectrum of Badachhape et al.[32] In an investigation of the effects of alkali metal and quaternary-ammonium cations on the rate of anodic formation of por-Si, white, sparingly soluble films formed on the external surface in the presence of K^+, Rb^+, and Cs^+. These were identified as hexafluorosilicates.[33,34] Stain etching of silicon in HF−oxidant−H_2O (oxidant = $K_2Cr_2O_7$, $KBrO_3$, or $KMnO_4$)

* Corresponding author: E-mail: k.w.kolasinski@qmul.ac.uk. Tel: +44-20 7882 3255. Fax: +44-20 7782 7794.

† School of Chemistry, The University of Birmingham.

‡ Current address: QinetiQ, St. Andrews Road, Malvern, Worcs WR14 3PS, U.K.

§ Nanoscale Physics Research Laboratory and the School of Physics and Astronomy, The University of Birmingham.

|| Current address: Laboratoire de Physique des Solides, UMR 5477, Université Paul Sabatier, 118 route de Narbonne, 31062 Toulouse Cedex 4, France.

⊥ Current address: Carl v. Ossietzky Universität Oldenburg, Fachbereich 9, Postfach 2503, D-2611 Oldenburg, Germany.

▽ Current address: Department of Chemistry, Queen Mary, University of London, Mile End Road, London E1 4NS, U.K.

10.1021/jp013213z CCC: $22.00
Published on Web 04/05/2002

TABLE 1: Sample Preparation Details Including Ranges of Time of Irradiation and Formal Concentrations of Etchants and Examination Techniques

designation of etchant	formal concentration (mol kg^{-1})	irradiation time (s)	examination techniques
pure HF(aq)	6.0−3.0 HF	1200−3600	SEM, PL, FTIR
NaF/HF	0.5 NaF + 0.5−6.0 HF	1000−2400	SEM, PL, FTIR
KHF_2	0.5−1.5 KHF_2	600−3600	SEM, PL, FTIR
KHF_2/HCl	1.0−3.0 KHF_2 + 1.0 HCl	600−4560	SEM, PL, FTIR
NH_4HF_2	2.0−6.0 NH_4HF_2	600−2400	SEM, PL, FTIR
HCl/HF	1.0 HCl + 3−6 HF	1800−4700	PL
KCl/HF	3.0−1.0 HF + 1.0−0.25 KCl	700−900	FTIR
RbCl/HF	6.0 HF + 3.0 RbCl	2400	PL, FTIR
CsF/HF	6.0 HF + 3.0 CsF	2400	PL, FTIR

has been studied.[35,36] As the concentration of the oxidant is increased, the etch rate increases to a limiting value as the thickness of the K_2SiF_6 increases. The layer thickens with reaction time until a point is reached when it stops further reaction by preventing the liquid reactants from making contact with the silicon surface. High HF concentrations (>12 M) are required to dissolve the K_2SiF_6 and further increase the etch rate. K_2SiF_6, therefore, has the ability to form a coating over the porous silicon that is insoluble not only in water but also in dilute HF(aq) and as such is a potential passivating agent.

In this study, por-Si is prepared by a photoelectrochemical technique, previously described,[37,38] without external bias. The holes necessary for etching are created by HeNe laser excitation. We have previously observed[39] a deposit on the external surface when potassium ions are present in the etchant. In this report, we identify the deposit as the hexafluorosilicate and determine whether the deposit is present on the internal surface. A significant blue shift of the PL peak and an intensity increase are observed for K_2SiF_6-coated films.

2. Experimental Section

The experimental apparatus is as described previously.[37,38] Samples of Si(111) of about 100 mm^2 and 0.5 mm thickness are cut from n-type (ρ = 4.5−10.4 Ω cm) silicon wafers, polished on one side. The Si and Teflon cell are cleaned in an ultrasonic bath in acetone and then with methanol, followed by thorough rinsing with deionized (DI) water. No external electrodes are attached to and no external bias is applied to the silicon, which is totally immersed in the etchant. The silicon is irradiated at normal incidence on the polished side using a 15 mW HeNe laser (633 nm, 1.96 eV), which exhibits a Gaussian intensity profile. The full width at half-maximum (fwhm) is 0.051 cm, resulting in a power density of 7.4 W cm^{-2}. Laser irradiation results in a temperature rise of <1 K. The etchants are made from HF(aq) (Fisher, electronics grade, 48% w/w), KHF_2 (Aldrich, 99%), NH_4HF_2 (Acros, 93%, contains up to 6% NH_4F), NaF (Fisher, >99%), HCl (Riedel de Haën, extra pure), CsF (Aldrich, 99%), RbCl (Aldrich, 99.8%), KCl (May and Baker, >99.5%), and DI according to Table 1. After irradiation, the silicon is rinsed in DI and ethanol and dried in a stream of nitrogen. The samples are handled and stored in air.

The por-Si was examined by scanning electron microscopy (SEM) at 5 kV. Features down to 5 nm can be resolved. Crystals on samples etched in KHF_2 were analyzed using energy dispersive X-ray analysis (EDX) in a SEM (20 kV). For transmission electron microscope analysis (top entry JEOL 200 CX TEM), the crystals are scratched off and transferred onto an electron-transparent amorphous carbon substrate on a copper support grid. Fourier transform infrared (FTIR) reflectance spectra were obtained with a Nicolet 760 FTIR spectrometer (300 scans, 2 cm^{-1} resolution) fitted with a microscope. Spatial resolution is provided by a 300 × 300 μm aperture.

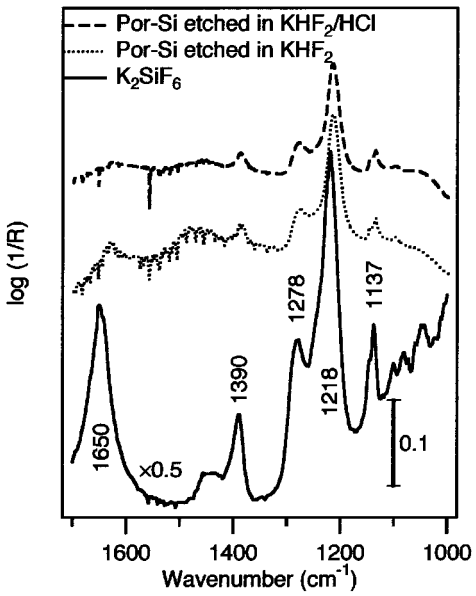

Figure 1. Reflection FTIR spectra of K_2SiF_6 and coated por-Si prepared in KHF_2 and in KHF_2/HCl.

A frequency-doubled Spectra Physics Tsunami fs Ti/sapphire laser or a Coherent FreD frequency-doubled argon ion laser is used for PL measurements. These systems provide various excitation wavelengths in the range of 244−488 nm (i.e., 5.08−2.54 eV). Plasma lines originating from the pump process in the lasers or remaining fundamental radiation are filtered out using a direct vision prism or dichroic mirrors. The excitation radiation is p polarized with respect to the sample. The sample is in air at room temperature and is illuminated by the slightly focused laser radiation under an angle of incidence of 15°. The emitted light is collected with an f = 50 mm camera lens and focused onto the entrance slit of a Jobin Yvon 0.25 m spectrometer. The spectrometer consists of a TRIAX190 single-grating monochromator with a nominal spectral resolution of 4 nm and a SPEX iCCD detector operating at a temperature of 240 K.

3. Results

3.1. Identification of Deposit. Por-Si prepared by the above technique in pure HF(aq), NaF/HF, and NH_4HF_2 appears dark; however, when K^+, Rb^+, or Cs^+ are present in the etchant, the irradiated area is initially dark but becomes white because of a polycrystalline deposit. This deposit is more readily formed when the etchant contains a high (2−3 mol kg^{-1}) formal concentration of K^+, Rb^+, or Cs^+, but deposits have been observed with formal concentrations down to 0.5 mol kg^{-1} if the silicon is irradiated for an extended time. Potassium-based etchants have been studied in the most detail, and unless stated otherwise, the following refers to K^+ and K_2SiF_6. It is reasonable to assume that Cs^+ and Rb^+ and their hexafluorosilicates are similar.

Evidence of other workers[31,33,35,36,40] suggests that the deposit is K_2SiF_6. EDX analysis of the crystals formed in KHF_2 shows that they contain silicon, potassium, and fluorine. FTIR shows bands at 1137, 1218, 1278, 1390, and 1650 cm^{-1} for the crystallites on the samples formed in KHF_2 and KHF_2/HCl (Figure 1), which correlates well with the published FTIR spectrum[32,41] of K_2SiF_6. FTIR spectra of the crystallites observed

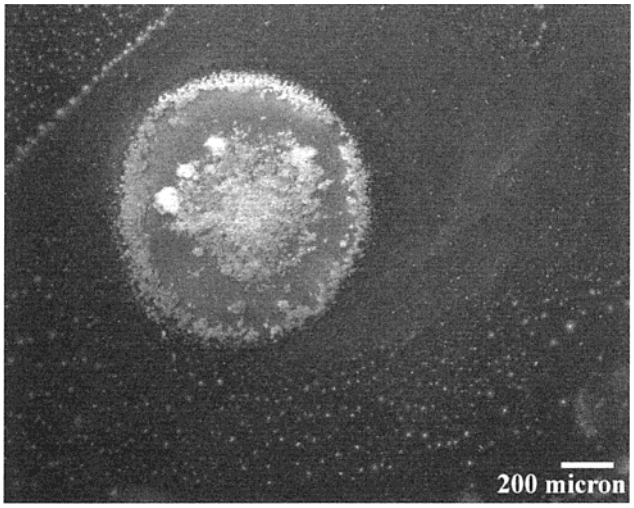

Figure 2. Plan view scanning electron micrographs of por-Si prepared in KHF_2 showing the annular ring and central layer of crystallites.

on por-Si formed in the etchants containing Cs^+ and Rb^+ display similar features to those of K_2SiF_6, shifted to lower wavenumber. We observe no similar features in this region for fresh por-Si formed in pure HF(aq), NaF/HF, or NH_4HF_2. TEM was performed on crystallites taken from the deposit. The selected area diffraction pattern of the crystal matches the K_2SiF_6 structure (space group $Fm\bar{3}m$, lattice constant 0.8134 nm).[42] Hence, the white crystallites are potassium, cesium, or rubidium hexafluorosilicate.

3.2. Location of Deposit. Plan view micrographs show that the crystallites often initially grow on the external surface as an annular ring at the extreme edge of the irradiated area (see Figure 2). Growth ensues in the center of the irradiated area initially as single crystals, agglomerating and expanding with time. With extended irradiation or high concentration of etchant, the entire area becomes covered with the deposit. The crystals are on top of the porous layer (Figure 3a) and penetrate into it such that accidental physical removal of a crystallite exposes a cavity in the porous layer (Figure 3b). Short irradiation or a relatively dilute etchant results in the formation of por-Si, but no crystallites are present.

From SEM evidence, hexafluorosilicates grow on the external surface but not in a uniform manner, spatially or temporally. To investigate the amount of hexafluorosilicate deposited as a function of time, the height of the strongest peak in the hexafluorosilicate spectrum (1218 cm^{-1}) is taken as a measure of the amount of deposit. An etchant made from HF(aq) and KCl was used so that the K^+ concentration was varied independently from the SiF_6^{2-} concentration, which is dependent on the etch rate (among other factors) and hence varies with the HF concentration. An induction time elapses before any hexafluorosilicate signal is detected. Detailed investigations into the temporal dependence of the induction period on K^+ or HF concentration have revealed that the induction period varies in a random fashion. For 0.25−1.0 M KCl and concentrations of HF from 1 to 3.0 mol kg^{-1}, the induction time ranges from 1700 to 4000 s; however, no reproducible correlation between these concentrations and the induction time could be found. FTIR spectra of por-Si etched for less than the induction period, which gave no deposit on the external surface, are all similar to each other, bear no resemblance to the spectrum of K_2SiF_6, but do resemble the spectrum of por-Si prepared in pure HF(aq).

3.3. Reactivity. The Si back-bond in H-terminated silicon starts to oxidize immediately on exposure to moist air, but complete oxidation under normal laboratory air takes weeks.[43] A broad band centered at 2085 cm^{-1}, attributed to $Si-H_x$, is observed from freshly prepared samples for all etchants with weaker bands between 2150 and 2250 cm^{-1} because of a small degree of oxidation (Figure 4a). After 10 days in air, three bands are observed that are centered at 2136, 2183, and 2235 cm^{-1} (Figure 4b), indicative of oxidation in the Si−Si back-bond. These agree well with previously recorded spectra of por-Si.[44−46] The rate of oxidation is the same with or without a deposit. Si−O transverse and longitudinal phonons are seen as two broad bands between 1100 and 1225 cm^{-1} in samples without crystallites, but these are less distinct in the presence of the hexafluorosilicate spectrum.

On exposure of a por-Si film to 1 M KOH(aq), fizzing is observed, which stops within 5 min. Porous silicon formed in pure HF(aq), NaF/HF, and NH_4HF_2 is totally removed, leaving a smooth, shallow depression in the surrounding silicon. When a polycrystalline deposit has been present, most is removed along with the por-Si, but some crystals often remain. Even when a thick layer of hexafluorosilicate is present, the por-Si is rapidly removed in cold KOH(aq), and no remnant of the hexafluorosilicate spectrum can be detected in the FTIR spectrum; only Si−O phonon bands are observed. Macroporous por-Si is more resistant to KOH(aq) than is microporous por-Si, KOH(aq) being used to remove microporous material from macropores.[47−49] A sample with a large number of crystallites (1.0 mol kg^{-1} KHF_2 for 2520 s) was examined by SEM after a short (∼1 min) dip in 1 M KOH(aq). Remaining crystallites, which have lost their original distinct facets, and areas from which crystallites have been removed are clearly visible (Figure 5a). Large pores (50−200 nm) remain at the edge of the spot (Figure 5b).

3.4. Photoluminescence. A motivating factor for this investigation was to produce por-Si with modified PL by deposition of a material within the porous layer. The deposited material can modify the PL signal either because it is itself luminescent or through changes induced by deposition. Air-dried thin films of por-Si prepared in 3−6 *m* HF(aq), NaF/HF, NaF/HCl, HCl/HF, and NH_4HF_2 photoluminesce in a broad peak centered at 642 ± 13 nm (Figure 6a). The peak is roughly Gaussian but is broadened on the low-energy side. The fwhm is roughly 110−120 nm. Films produced in KHF_2 that are not coated with a deposit also exhibit a similar PL spectrum. Sample-to-sample variations made it impossible to differentiate the PL behavior among these films. Nonetheless, the PL spectra from these films are blue-shifted compared to films produced in 48% (w/w) HF(aq), which luminesce at 677 ± 18 nm.[16] The peak shape and width are similar in all instances. Such spectra are typical of air-dried samples with porosity in the range 70−90%.[13] Porosity measurements carried out on films etched in 48% HF(aq) confirm this value.[50]

When crystallites are visible on the surface of the por-Si, the PL has a peak at 611 ± 12 nm or 593 ± 18 nm for films produced in KHF_2 (Figure 6b) or KHF_2/HCl, respectively. The peak PL wavelength for Rb and Cs hexafluorosilicate deposits falls within the range of samples with deposits produced in KHF_2. No PL is visible on any sample after treatment with KOH(aq). The question is now whether the deposit leads to the PL shift directly, as a results of its own photoluminescence, or indirectly, from some effect on film properties (structure, dielectric constant, etc.). Consistent with a prior report,[51] we find that pure K_2SiF_6 does not luminesce significantly in the

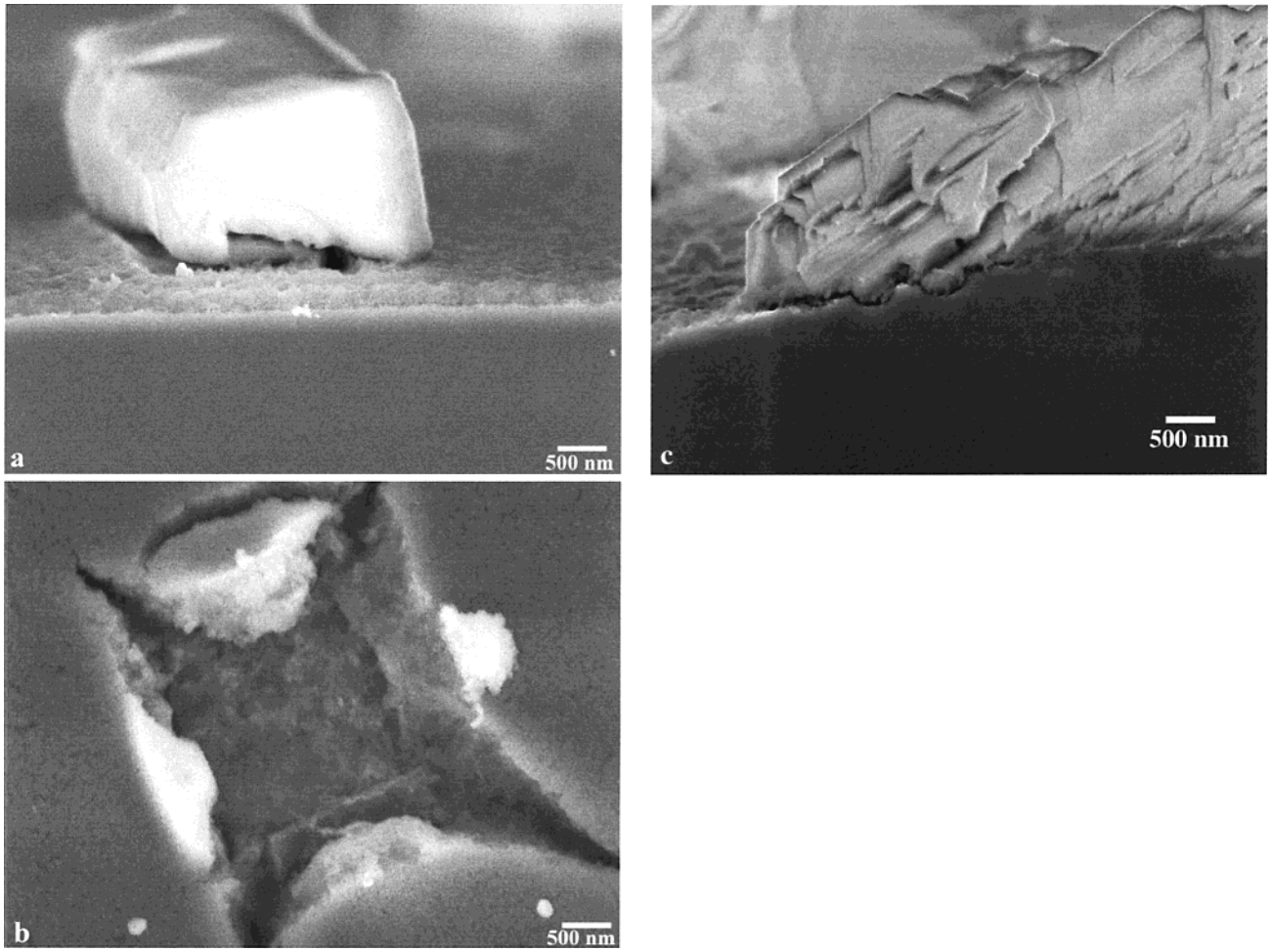

Figure 3. Scanning electron micrographs of por-Si prepared in KHF_2. (a) A crystallite embedded in the porous layer (plan view). (b) A cavity in the porous layer where a crystallite has been accidentally removed (plan view). (c) Intimate contact at the K_2SiF_6/Si interface (cross section).

visible under UV excitation. Therefore, it cannot be the source of the PL spectrum from films with a deposit.

4. Discussion

4.1. Deposition of A_2SiF_6(A = K, Cs, Rb). A polycrystalline deposit is observed only when K^+, Rb^+, or Cs^+ is present in the etchant at sufficiently high concentration. The properties of por-Si will depend on the location of the deposit, and here we determine whether the crystallites form on the external or internal surface or on some combination of the two.

The characteristic bands of the hexafluorosilicates, Figure 1, are not seen in the IR spectra unless crystals are visible on the external surface of the por-Si. Further IR data demonstrate that hexafluorosilicates are not deposited continuously during etching but only after an induction period. SEM micrographs (Figure 3) show crystals on top of and embedded in por-Si, but we find no evidence that K_2SiF_6 grows as a layer on the internal surface. Instead, K_2SiF_6 crystallites form 3D islands. The intimate contact at the K_2SiF_6/Si interface and strong adhesion of the overlayer indicate that deposition occurs via heterogeneous nucleation of crystallites rather than via precipitation from solution. Crystallites do not halt etching, which demonstrates that the etchant can access the silicon beneath the crystallite. Etching continues under and around the crystallites, providing SiF_6^{2-} for 3D growth. Extensive cross-sectional SEM studies have failed to find more than a thin (~100 nm) film of por-Si under the crystallite layer even with extended etching, whereas films of 1 μm are readily formed in HF(aq). The external surface is covered with the deposit as more crystallites aggregate.

The processes involved in the laser-assisted etching of n-type Si in fluoride solutions are illustrated in Figure 7. Assuming equivalence between electrochemical and laser-assisted etching, several aspects of Figure 7 are unassailable: (1) a hole captured at the surface initiates etching,[52] (2) defects enhance the initiation of etching,[38,53] (3) H_2 is a product,[54] (4) electron injection into the Si occurs,[55−57] (5) the Si is predominantly H-terminated before, during, and after electrochemical etching[58−60] (6) SiF_6^{2-} is a byproduct, (7) in the presence of K^+, Rb^+, and Cs^+, hexafluorosilicate deposition can occur,[34,61] (8) the counter reaction occurs in a spatially separated region of the crystal,[38] and (9) both HF and HF_2^- can react with the Si atom to be etched.[62] Several aspects are probable but remain to be proved unequivocally: (1) a H^+ desorbs after hole capture at the surface,[53] (2) a F^- attacks the empty site,[53,57,63] and (3) the primary etch product reacts with HF to form SiF_6^{2-}.[53] Some aspects remain unclear: (1) whether OH^- or H_2O plays a direct role in the reactions, (2) whether $HSiF_3$ is the primary etch product, (3) whether the counter reaction involves solely the reduction of hydrogen ions or if dissolved oxygen is involved, and (4) several mechanistic details that distinguish the mechanism of Gerischer, Allongue, and Costa Kieling[53] from those of Kooij and Vanmaekelbergh,[57] Lehmann and Gösele,[63] and Kang and Jorné.[64]

K_2SiF_6 deposition does not occur continuously in a layer-by-layer mode; rather, it deposits only after the delayed

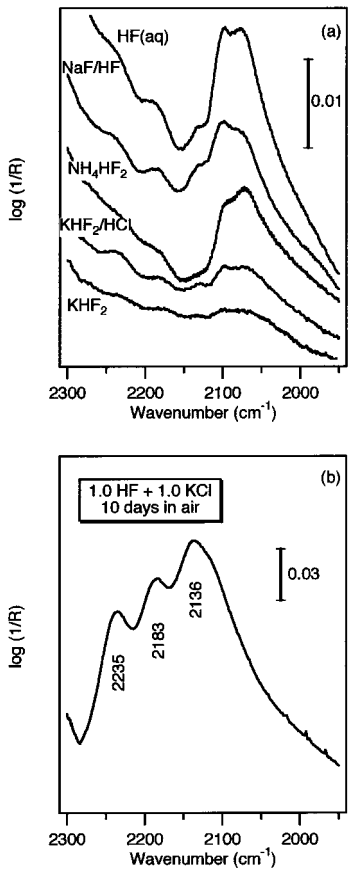

Figure 4. Reflection FTIR spectra of the Si−H_x stretching region after (a) ∼1 h and (b) 10 days in air. The region near 2085 cm^{-1} is indicative of the Si−H_x species in the absence of oxygen. Thus, the spectra in (a) demonstrate H termination of por-Si made in all five etchants. The shift of the peaks displayed in (b) is indicative of insertion of O into the Si back-bonds. Film depth varies between samples, thus intensities cannot be compared quantitatively.

formation of nucleation centers, followed by Volmer−Weber growth. A necessary condition for deposition, therefore, is that a sufficient concentration of SiF_6^{2-} builds up such that the solubility product of K_2SiF_6 (6.3×10^{-7} mol^3 dm^{-9})[65] is exceeded. For a typical Gaussian spot, the depth of which is described by $d(r) = d_{max} \exp(^{-r^2}/_{2\sigma^2})$ with $d_{max} = 1.61 \times 10^{-7}$ m and $s = 2.17 \times 10^{-4}$ m, only $\sim 1 \times 10^{-12}$ mol of Si is removed by etching. This is far too low a value to exceed the solubility product for a well-mixed solution. However, we rely solely upon diffusion for mass transport in the solution. Using the kinetics of reaction and diffusion,[66−68] we are able to estimate the concentrations of the fluoride solution species.

We have calculated the concentration profiles assuming a uniform reaction rate across the spot corresponding to the maximum reaction rate at the center of the spot. This is a strict upper bound to the experimental situation because the reaction rate decreases as a 2D Gaussian away from the center of the spot. The solution to the reaction−diffusion equation can be adapted from results found elsewhere.[67] The fastest etching rate that we have observed is 1.5 nm s^{-1} for both 6 *m* HF(aq) and 1 *m* KHF_2(aq).[62] This rate corresponds to a Si atom removal rate of $R_{Si} \approx 7.5 \times 10^{19}$ m^{-2} s^{-1} (∼9.6 ML s^{-1} where 1 ML is the areal density referred to that of an ideal Si(111) plane). We find that even this highest reaction rate is so slow compared to the diffusion rate that no appreciable (<0.3%) depletion of the HF or K^+ concentrations at the surface occurs.

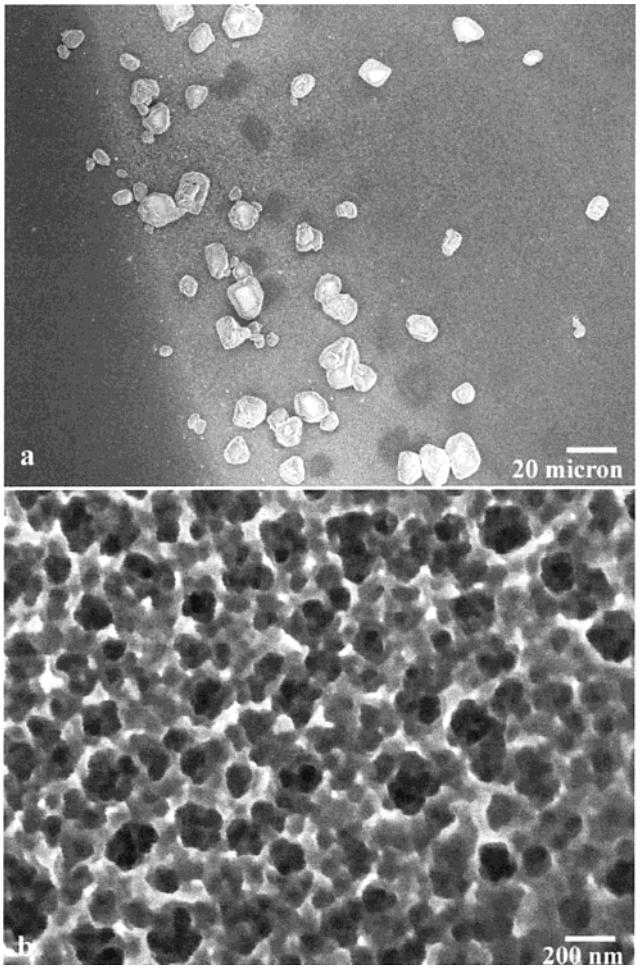

Figure 5. Plan view scanning electron micrographs of crystallites and por-Si formed in KHF_2 after ∼1 min of treatment with KOH. (a) The K_2SiF_6 crystallites lose their distinct facets after exposure to KOH. (b) Por-Si at the edge of the irradiated area. Brief exposure to KOH removes nanoporous Si and leads to morphological changes in both the crystallites and the por-Si layer.

The concentration profile of SiF_6^{2-} is found by adapting the solution of Oosterkamp[69,70] for heat flow from a uniformly heated circular spot. This profile represents an upper limit to the true value at the center of the spot as the flux of SiF_6^{2-} decreases in a Gaussian fashion away from the center. Assuming that the primary etch product is hydrolyzed completely to SiF_6^{2-} inside of the pores and that all of the SiF_6^{2-} reaches the exterior surface of the por-Si, the flux of SiF_6^{2-} at the center of the spot is equal to the flux of Si atoms liberated by etching, which results in a calculated SiF_6^{2-} concentration of 4.6×10^{-6} mol dm^{-3}. Because the K^+ concentration in this experiment is 1 mol dm^{-3}, the concentration at which K_2SiF_6 precipitates is 6.3×10^{-7} mol dm^{-3}. As the calculated concentration exceeds this value, we predict that K_2SiF_6 can precipitate, consistent with our results. Rb_2SiF_6 and Cs_2SiF_6 have lower solubilities whereas Na_2SiF_6 and $(NH_4)_2SiF_6$ have higher solubilities than does K_2SiF_6. Consistent with experimental results, our calculations predict that the former two will precipitate whereas the latter two will not.

When K_2SiF_6 is synthesized in aqueous solution, it forms a colloid that does not spontaneously deposit.[71] Any particles settling on the surface would wash off easily whereas the deposit, once formed, is strongly bound to the surface. Chemical removal of a native oxide layer from a planar surface in quiescent KHF_2 can lead to local concentrations of K^+ and

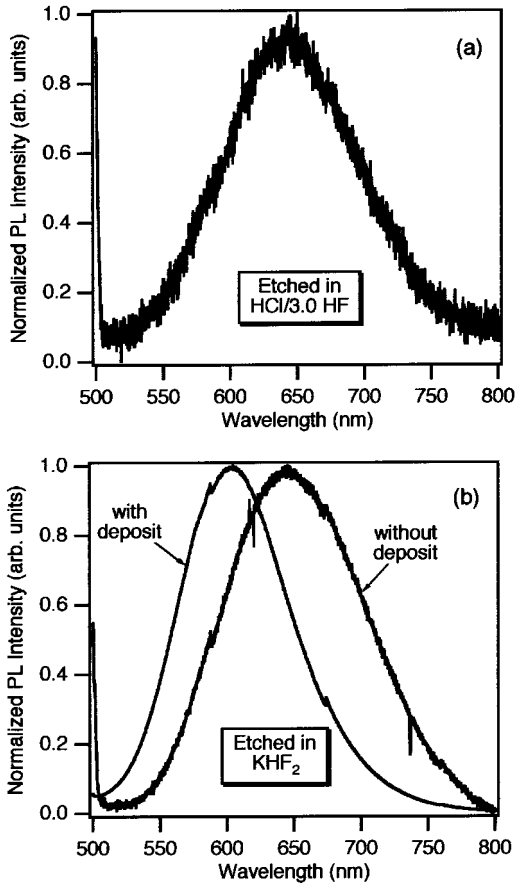

Figure 6. Photoluminescence spectra. (a) Por-Si prepared in 1.0 *m* HCl + 3.0 *m* HF. This spectrum (peak emission at 642 ± 13 nm) is typical of all films except those that are (i) covered by a deposit (590−610 nm) or (ii) etched in 48% HF(aq) (677 ± 18 nm). (b) Por-Si formed in KHF_2(aq) with and without a deposit.

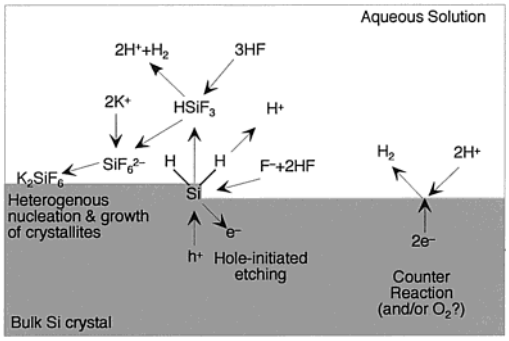

Figure 7. Illustration of the processes occurring during laser-assisted etching of Si in an alkali metal-containing fluoride solution. The processes include anodic etching and the cathodic counter reaction and hydrolysis of the primary etch product and heterogeneous deposition of K_2SiF_6.

SiF_6^{2-} that are similar to those calculated in the above example. Nonetheless, we do not observe deposition onto a planar surface under these circumstances. Thus, the nucleation of K_2SiF_6 crystallites is *a heterogeneous process that is sensitive to surface structure and not just to concentration.* Por-Si surfaces are especially well-suited for the formation of nucleation centers. The use of por-Si as a source of nucleation sites has been previously reported for calcium phosphate[2] and diamond.[72]

The following model describes the growth of K_2SiF_6. Porous silicon is continually being formed and is accompanied by the production of SiF_6^{2-} because of the hydrolysis of the primary etch product. This hydrolysis reaction is sufficiently rapid that much, if not all, of the SiF_6^{2-} is produced during the time it takes the etch product to diffuse through the porous layer. As etching proceeds, pores are formed, and the concentration of SiF_6^{2-} near the mouths of the pores builds up to a sufficient extent to exceed the solubility of K_2SiF_6. K_2SiF_6 then nucleates heterogeneously near the mouths of the pores. After nucleation, the crystallites continuously grow in three dimensions. Growth can also proceed down into the pore beneath the crystallite and is not necessarily impeded when the crystallite grows to the same dimension as the pore mouth that it occupies.

It remains to ask why the distribution of the crystallites over the irradiated area is not uniform, particularly that of the annular ring. The SiF_6^{2-} concentration should vary in a radially regular way, depending on the rates of formation and diffusion, across the irradiated area. Certainly, a high concentration at the very edge of this area is not anticipated. This is the region where the rate of etching is slowest, and hence the rate of formation of SiF_6^{2-} is slowest. However, it is here where the crystallites are often first seen, so there must be some inhomogeneity causing the first deposition to occur in this area. When the annular ring forms, the etching process is well-established, and it is expected that a depth approaching 100 nm of por-Si is present. The porous structure is not uniform across the irradiated area; rather, pores of increasing diameter are found toward the edge of the spot.[73] This inhomogeneous structure must account for the annular ring, wide pores being more accommodating to nucleation than narrow ones.

4.2. Blue-Shifted PL in the Presence of Hexafluorosilicate. In the absence of a hexafluorosilicate deposit on the external surface, the PL spectrum for por-Si formed in the presence of K^+ is the same as that for por-Si formed in pure HF(aq), HCl/HF, and all other solutions that do not lead to a deposit (Figure 6). This is consistent with the evidence from FTIR and SEM that no K^+ or K_2SiF_6, which might be expected to alter the light emission characteristics of the por-Si, deposits on the internal surface before deposition on the external surface. When a deposit is visible on the external surface, the PL peak is blue-shifted, corresponding to emission in the presence of K_2SiF_6. The PL intensity of a coated film is significantly greater than that of an uncoated film. Qualitatively, this intensity difference can be seen in Figure 6b by noting the reduced signal-to-noise ratio of the uncoated film compared to that of the coated film. Quantitative comparisons are not possible in the absence of knowledge of how K_2SiF_6 affects the absorption of laser light. Because K_2SiF_6 does not luminesce significantly in the visible, we assign the source of the PL in a deposit-covered film to the por-Si rather than to the deposit. The blue shift might arise from a change in the effective dielectric constant of the film because of the presence of the deposit. Such a shift has been previously observed for por-Si films in various organic solvents[74] as well as for por-Si immersed in HF(aq), as compared to the luminescence of por-Si in an Ar atmosphere.[16] This could be at the root of the PL peak shift observed here and suggests that by choice of dielectric material the peak emission wavelength of por-Si composite films can be shifted through the visible. Such an explanation based on effective medium approximations, however, seemingly requires the K_2SiF_6 to be distributed uniformly throughout the film. We do not observe a uniform distribution. Alternatively, the emission may be associated with a defect state inherent to the K_2SiF_6/Si interface. The involvement of surface states in photoluminescence from SiO_2/Si interfaces has received both experimental[75,76] and theoretical verification.[77] The formation of the CaF_2/Si interface is also associated with the formation of interface states,[78] and it has

been suggested that they too could be involved in radiative transitions.[79] The involvement of surface states in the PL observed from K_2SiF_6/por-Si appears to be the more likely explanation because of the nonuniform K_2SiF_6 distribution. This explanation requires the K_2SiF_6/por-Si interface emitter state to be particularly efficient because the PL efficiency of coated films is greater than that of uncoated films of similar depth.

5. Conclusions

Cubic crystallites of hexafluorosilicates are formed within and over the por-Si layer during etching from K^+, Rb^+, or Cs^+ and the etch product SiF_6^{2-}. The deposition of hexafluorosilicates occurs via heterogeneous nucleation and growth of crystallites rather than from simple precipitation out of solution. The blue-shifted photoluminescence in the presence of the hexafluorosilicate (from ~640 to ~600 nm) is associated with modified emission from the porous silicon rather than from the hexafluorosilicate. By using this laser-assisted route, it is possible to deposit hexafluorosilicates and modify the photoluminescence of porous silicon in an area-selective manner without the use of masking.

Acknowledgment. We acknowledge EPSRC for financial support and the provision of studentships (L.K. and A.W.). We thank Leigh Canham for assistance with EDX measurements. R.N. was supported by a Marie Curie Fellowship of the European Commission. The FreD laser used in PL measurements was provided by the EPSRC Laser Loan Pool.

References and Notes

(1) Canham, L. T. *Appl. Phys. Lett.* **1990**, *57*, 1046.
(2) Canham, L. T.; Reeves, C. L.; Wallis, D. J.; Newey, J. P.; Houlton, M. R.; Sapsford, G. J.; Godfrey, R. E.; Loni, A.; Simons, A. J.; Cox, T. I.; Ward, M. C. L. *Mater. Res. Soc. Symp. Proc.* **1997**, *452*, 579.
(3) Li, X.; Coffer, J. L.; Chen, Y.; Pinizzotto, R. F.; Newey, J.; Canham, L. T. *J. Am. Chem. Soc.* **1998**, *120*, 11706.
(4) Bowditch, A. P.; Waters, K.; Gale, H.; Rice, P.; Scott, E. A. M.; Canham, L. T.; Reeves, C. L.; Loni, A.; Cox, T. I. *Mater. Res. Soc. Symp. Proc.* **1999**, *576*, 149.
(5) Arrand, H. F.; Benson, T. M.; Loni, A.; Arens-Fischer, R.; Krüger, M.; Thönissen, M.; Lüth, H.; Kershaw, S. *IEEE Photonics Technol. Lett.* **1998**, *10*, 1467.
(6) Foucaran, A.; Pascal-Delannoy, F.; Giani, A.; Sackda, A.; Combette, P.; Boyer, A. *Thin Solid Films* **1997**, *297*, 317.
(7) Hilbrich, S.; Arens-Fischer, R.; Küppers, L.; Theiβ, W.; Berger, M. G.; Krüger, M.; Thönissen, M. *Thin Solid Films* **1997**, *297*, 250.
(8) Janshoff, A.; Dancil, K.-P. S.; Steinem, C.; Greiner, D. P.; Lin, V. S.-Y.; Gurtner, C.; Motesharei, K.; Sailor, M. J.; Ghadiri, M. R. *J. Am. Chem. Soc.* **1998**, *120*, 12108.
(9) Lin, V. S.-Y.; Motesharei, K.; Dancil, K.-P. S.; Sailor, M. J.; Ghadiri, M. R. *Science* **1997**, *278*, 840.
(10) Snow, P. A.; Squire, E. K.; Russell, P. S. J.; Canham, L. T. *J. Appl. Phys.* **1999**, *86*, 1781.
(11) Prokes, S. M. *J. Mater. Res.* **1996**, *11*, 305.
(12) Calcott, P. D. J.; Nash, K. J.; Canham, L. T.; Kane, M. J.; Brumhead, D. *J. Lumin.* **1993**, *57*, 257.
(13) Cullis, A. G.; Canham, L. T.; Calcott, P. D. J. *J. Appl. Phys.* **1997**, *82*, 909.
(14) Ozanam, F.; Chazalviel, J.-N.; Wehrspohn, R. B. *Thin Solid Films* **1997**, *297*, 53.
(15) Chang, I. M.; Chen, Y. F. *J. Appl. Phys.* **1997**, *82*, 3514.
(16) Kolasinski, K. W.; Aindow, M.; Barnard, J. C.; Ganguly, S.; Koker, L.; Wellner, A.; Palmer, R. E.; Field, C.; Hamley, P.; Poliakoff, M. *J. Appl. Phys.* **2000**, *88*, 2472.
(17) Kolasinski, K. W.; Barnard, J. C.; Koker, L.; Ganguly, S.; Palmer, R. E. *Mater. Sci. Eng., B* **2000**, *69*−*70*, 156.
(18) Andsager, D.; Hilliard, J.; Hetrick, J. M.; AbuHassan, L. H.; Plisch, M.; Nayfeh, M. H. *J. Appl. Phys.* **1993**, *74*, 4783.
(19) Andsager, D.; Hilliard, J.; Nayfeh, M. H. *Appl. Phys. Lett.* **1994**, *64*, 1141.
(20) Li, X. J.; Zhang, Y. H. *Phys. Rev. B: Condens. Matter* **2000**, *61*, 12605.
(21) Gorostiza, P.; Díaz, R.; Kulandainathan, M. A.; Sanz, F.; Morante, J. R. *J. Electroanal. Chem.* **1999**, *469*, 48.
(22) Wu, X.; Hömmerich, U.; Namavar, F.; Cremins-Costa, A. M. *Appl. Phys. Lett.* **1996**, *69*, 1903.
(23) Hömmerich, U.; Namavar, F.; Cremins, A.; Bray, K. L. *Appl. Phys. Lett.* **1996**, *68*, 1951.
(24) Ng, W. L.; Temple, M. P.; Childs, P. A.; Wellhofer, F.; Homewood, K. P. *Appl. Phys. Lett.* **1999**, *75*, 97.
(25) Hérino, R. *Mater. Sci. Eng., B* **2000**, *69*−*70*, 70.
(26) Buriak, J. M. *Chem. Commun.* **1999**, 1051.
(27) Buriak, J. M. *Adv. Mater. (Weinheim, Ger.)* **1999**, *11*, 265.
(28) Ben Ali, M.; Mlika, R.; Ben Ouada, H.; M'ghaieth, R.; Maaref, H. *Sens. Actuators, A* **1999**, *74*, 123.
(29) Thust, M.; Schöning, M. J.; Schroth, P.; Malkoc, U.; Dicker, C.; Steffen, A.; Kordos, P.; Lüth, H. *J. Mol. Catal. B: Enzym.* **1999**, *7*, 77.
(30) Angelucci, R.; Poggi, A.; Dori, L.; Cardinali, G. C.; Parisini, A.; Tagliani, A.; Mariasaldi, M.; Cavani, F. *Sens. Actuators, A* **1999**, *74*, 95.
(31) Boyle, D. S.; Chudek, J. A.; Hunter, G.; James, D.; Littlewood, M. I.; McGhee, L.; Robertson, M. I.; Winfield, J. M. *J. Mater. Chem.* **1993**, *3*, 903.
(32) Badachhape, R. B.; Hunter, G.; McCory, L. D.; Margrave, J. L. *Inorg. Chem.* **1966**, *5*, 929.
(33) Hassan, H. H.; Chazalviel, J.-N.; Neumann-Spallart, M.; Ozanam, F.; Etman, M. *J. Electroanal. Chem.* **1995**, *381*, 211.
(34) Hassan, H. H.; Fotouhi, B.; Sculfort, J.-L.; Abdel-Rehiem, S. S.; Etman, M.; Ozanam, F.; Chazalviel, J.-N. *J. Electroanal. Chem.* **1996**, *407*, 105.
(35) Seo, Y. H.; Nahm, K. S.; Lee, K. B. *J. Electrochem. Soc.* **1993**, *140*, 1453.
(36) Nahm, K. S.; Seo, Y. H.; Lee, H. J. *J. Appl. Phys.* **1997**, *81*, 2418.
(37) Koker, L.; Kolasinski, K. W. *J. Appl. Phys.* **1999**, *86*, 1800.
(38) Koker, L.; Kolasinski, K. W. *Phys. Chem. Chem. Phys.* **2000**, *2*, 277.
(39) Wellner, A.; Koker, L.; Kolasinski, K. W.; Aindow, M.; Palmer, R. E. *Phys. Status Solidi A* **2000**, *182*, 87.
(40) Hassan, H. H.; Sculfort, J. L.; Etman, M.; Ozanam, F.; Chazalviel, J.-N. *J. Electroanal. Chem.* **1995**, *380*, 55.
(41) Prinsloo, L. C.; Heyns, A. M.; Ehrl, R.; Range, K. J. *Eur. J. Solid State Inorg. Chem.* **1997**, *34*, 881.
(42) Loehlin, J. H. *Acta Crystallogr.* **1984**, *C40*, 570.
(43) Miura, T.-a.; Niwano, M.; Shoji, D.; Niyamoto, N. *J. Appl. Phys.* **1996**, *79*, 4373.
(44) Ogata, Y.; Niki, H.; Sakka, T.; Iwasaki, M. *J. Electrochem. Soc.* **1995**, *142*, 195.
(45) Tischler, M. A.; Collins, R. T. *Solid State Commun.* **1992**, *84*, 819.
(46) Ogata, Y.; Niki, H.; Sakka, T.; Iwasaki, M. *J. Electrochem. Soc.* **1995**, *142*, 1595.
(47) Lévy-Clément, C.; Lagoubi, A.; Tomkiewicz, M. *J. Electrochem. Soc.* **1994**, *141*, 958.
(48) Schöning, M. J.; Ronkel, F.; Crott, M.; Thust, M.; Schultze, J. W.; Kordos, P.; Lüth, H. *Electrochim. Acta* **1997**, *42*, 3185.
(49) Lehmann, V.; Föll, H. *J. Electrochem. Soc.* **1990**, *137*, 653.
(50) Lee, C.; Koker, L.; Kolasinski, K. W. *Appl. Phys. A: Mater. Sci. Process.* **2000**, *71*, 77.
(51) Kröger, F. A. *Some Aspects of the Luminescence of Solids*; Elsevier: New York, 1948.
(52) Smith, R. L.; Collins, S. D. *J. Appl. Phys.* **1992**, *71*, R1.
(53) Gerischer, H.; Allongue, P.; Costa Kieling, V. *Ber. Bunsen-Ges. Phys. Chem.* **1993**, *97*, 753.
(54) Stumper, J.; Peter, L. M. *J. Electroanal. Chem.* **1991**, *309*, 325.
(55) Peter, L. M.; Borazio, A. M.; Lewerenz, H. J.; Stumper, J. *J. Electroanal. Chem.* **1990**, *290*, 229.
(56) Matsumura, M.; Morrison, S. R. *J. Electroanal. Chem.* **1983**, *147*, 157.
(57) Kooij, E. S.; Vanmaekelbergh, D. *J. Electrochem. Soc.* **1997**, *144*, 1296.
(58) Doan, V. W.; Penner, R. M.; Sailor, M. J. *J. Phys. Chem.* **1993**, *97*, 4505.
(59) Peter, L. M.; Blackwood, D. J.; Pons, S. *Phys. Rev. Lett.* **1989**, *62*, 308.
(60) Rappich, J.; Lewerenz, H. J. *Electrochim. Acta* **1996**, *41*, 675.
(61) Burrows, V. A.; Yota, J. *Thin Solid Films* **1990**, *193*−*194*, 371.
(62) Koker, L.; Kolasinski, K. W. *J. Phys. Chem. B* **2001**, *105*, 3864.
(63) Lehmann, V.; Gösele, U. *Appl. Phys. Lett.* **1991**, *58*, 856.
(64) Kang, Y.; Jorné, J. *Electrochim. Acta* **1998**, *43*, 2398.
(65) *CRC Handbook of Chemistry and Physics*; Weast, R. C., Ed.; CRC Press: Boca Raton, FL, 1980; Vol. 60.

(66) Noulty, R. A.; Leaist, D. G. *Electrochim. Acta* **1985**, *30*, 1095.
(67) Carslaw, H. S.; Jaeger, J. C. *Conduction of Heat in Solids*; Clarendon Press: Oxford, 1959.
(68) Crank, J. *The Mathematics of Diffusion*; Clarendon Press: Oxford, 1975.
(69) Oosterkamp, W. J. *J. Appl. Phys.* **1948**, *19*, 1181.
(70) Oosterkamp, W. J. *Philips Res. Rep.* **1948**, *3*, 49.
(71) Koker, L.; Jones, M. O.; Kolasinski, K. W. Unpublished work.
(72) Baranauskas, V.; Tosin, M. C.; Peterlevitz, A. C.; Ceragioli, H. J.; Durrant, S. F. *Mater. Sci. Eng., B* **2000**, *69*−*70*, 171.
(73) Koker, L.; Wellner, A.; Sherratt, P. A. J.; Neuendorf, R.; Kolasinski, K. W. *Phys. Status Solidi A*, submitted for publication.
(74) Chazalviel, J.-N.; Ozanam, F.; Dubin, V. M. *J. Phys. I* **1994**, *4*, 1325.
(75) Wolkin, M. V.; Jorne, J.; Fauchet, P. M.; Allan, G.; Delerue, C. *Phys. Rev. Lett.* **1999**, *82*, 197.
(76) Wellner, A.; Palmer, R. E.; Zheng, J. G.; Kiely, C. J.; Kolasinski, K. W. *J. Appl. Phys.* **2002**, *91*, 3294.
(77) Delerue, C.; Lannoo, M.; Allan, G. *Phys. Rev. Lett.* **2000**, *84*, 2457.
(78) Heinz, T. F.; Himpsel, F. J.; Palange, E.; Burstein, E. *Phys. Rev. Lett.* **1989**, *63*, 644.
(79) Ossicini, S.; Fasolino, A.; Bernardini, R. *Phys. Rev. Lett.* **1994**, *72*, 1044.